Variant of the anastigmatic telescope with three mirrors for back focal length

J. Herrera,[1,*] S. Vázquez,[2] E. Luna,[1] L. Salas,[1] J. Nuñez,[1] E. Sohn,[1] and E. Ruiz[1]

[1]Universidad Nacional Autonoma de México, Instituto de Astronomía, Observatorio Astronomico Nacional. Apdo. Postal 877, Ensenada, B. C. 22800, Mexico

[2]Instituto Nacional de Astrofisica, Óptica y Electrónica, Luis Enrique Erro # 1, Tonantzintla, Puebla, Mexico

*Corresponding author: joel@astrosen.unam.mx

Received 23 September 2010; revised 15 December 2010; accepted 16 December 2010; posted 21 December 2010 (Doc. ID 135515); published 28 April 2011

In this paper, an optical design is presented for an anastigmatic telescope with back focal length corrected with exact ray tracing to eliminate spherical, coma, and astigmatism aberrations. The telescope is formed of three conical mirrors, two of them polished on the same substratum. The optical design is divided into three stages: we began the design obtaining the Gaussian parameters in a first-order solution; posteriorly, were obtained analytically the three mirrors' asphericity in a third-order design. The final design stage consists of the implementation of the Fermat's principle, the Abbe sine condition, and the Coddington equations for the exact correction for the three aforementioned aberrations.

OCIS codes: 110.6770, 220.4830, 080.2740.

1. Introduction

The present work shows the design of a very particular compact telescope using three conical mirrors. Some authors, such as Korsch [1] and Robb [2], have studied the third-order correction for anastigmatic systems with three mirrors; this idea has been widely used in the design of anastigmatic systems. We present a methodology to obtain the system parameters in an exact way for a configuration with three mirrors and four reflections; in addition, we show an analytical third-order solution for this particular configuration.

There exist some configurations of telescopes with three mirrors like the large synoptic survey telescope [3], where the focal plane is located in front of the primary mirror. The configuration shown in this paper provides a posterior, or back focal length.

To start our design, we use a compact Gregory telescope [4]; a Gregory telescope can be bent using a flat mirror between the secondary and the primary mirror. With this modification, the secondary and the primary are located in the same space, making the construction of both elements in the same substratum possible, obtaining a compact Gregory telescope.

If we change the flat mirror by a curved mirror, we can use the asphericity as variables in the system correction. We propose three equations, one for each optical aberration. The variable value of these equations is the asphericity, ε, of each mirror. The powers B_i, positions d_i, and diameters D_i were obtained by means of the matrix-based ray trace [5]. In this stage, the $F/\# = F_{\text{total}}/D_1$ and the working distance d_w of the telescope are defined.

For the third-order design, the Seidel sums have been calculated obtaining three equations in term of the asphericity ε; these equations can be solved simultaneously for zero sum values to obtain the third-order corrected system. We used Fermat's principle [6], the Abbe sine condition [7], Coddington equations [8], and the skew ray tracing [6] to built the functions corresponding to the correction of each aforementioned aberration.

In this system, a ray is reflected four times, which complicates the explicit expression of the required

0003-6935/11/131905-10$15.00/0

equations, but it is easy to use algorithms with the ray tracing that represent the three principles before mentioned. The three functions can be solved simultaneously with the three dimensional Newton–Raphson method using the third-order asphericity as the initial values.

2. First-Order Design

To calculate the Gaussian parameters, we use the system shown in Fig. 1, where for simplicity, the powers ($B_1 = 1/f_1, B_2 = 1/f_2, B_3 = 1/f_3$) and the separations are positive values. In practice, f_1 and f_2 will correspond to positive focal lengths of concave mirrors, and f_3 will be negative to minimize the Petzval curvature.

The elements with powers B_2, represent the same mirror. In this case, the secondary mirror is located a distance d_2 from the tertiary mirror, which is integrated to the primary mirror. From Fig. 1, we obtain the system matrix of Eq. (1):

$$\begin{pmatrix} a & b \\ c & d \end{pmatrix} = \begin{pmatrix} 1 & -\frac{1}{f_2} \\ 0 & 1 \end{pmatrix}\begin{pmatrix} 1 & 0 \\ d_2 & 1 \end{pmatrix}\begin{pmatrix} 1 & -\frac{1}{f_3} \\ 0 & 1 \end{pmatrix}\begin{pmatrix} 1 & 0 \\ d_2 & 1 \end{pmatrix} \times \begin{pmatrix} 1 & -\frac{1}{f_2} \\ 0 & 1 \end{pmatrix}\begin{pmatrix} 1 & 0 \\ d_1 & 1 \end{pmatrix}\begin{pmatrix} 1 & -\frac{1}{f_1} \\ 0 & 1 \end{pmatrix}, \quad (1)$$

where the value of b is the power of the total system, hence,

$$-b^{-1} = F_{\text{total}} = \frac{-f_1 f_2^2 f_3}{A + B + C}, \quad (2)$$

where

$$\begin{aligned} A &= f_2^2(f_1 - d_1 + f_3) + d_2^2(f_1 - d_1 + f_2), \\ B &= -d_2(f_2(f_2 + 2(f_1 - d_1 + f_3)) + 2f_3(f_3 - d_1)), \\ C &= 2f_2 f_3(f_1 - d_1). \end{aligned} \quad (3)$$

A. Working Distance

During the design, it is necessary to establish the working distance d_w, which is the distance from the last element vertex to the image plane. If we trace a parallel ray to the optical axis, this ray must yield the optical axis at the image-plane position. To ensure the working distance, we modify the system matrix adding the separation "$d_2 + d_w$," so the matrix will be redefined by

$$\begin{pmatrix} a' & b' \\ c' & d' \end{pmatrix} = \begin{pmatrix} 1 & 0 \\ d_2 + d_w & 1 \end{pmatrix}\begin{pmatrix} a & b \\ c & d \end{pmatrix}. \quad (4)$$

The working-distance condition is determined by the following equation:

$$\begin{pmatrix} a' & b' \\ c' & d' \end{pmatrix} = \begin{pmatrix} a & b \\ c & d \end{pmatrix}\begin{pmatrix} \theta_{\text{in}} \\ h \end{pmatrix}. \quad (5)$$

Equation (5) guarantees that an incident ray with an angle $\theta_{\text{in}} = 0$ and a height of incidence, h, will be equal to zero at the working distance. Hence, from Eq. (5) we have

$$d' = 0, \quad (6)$$

where the value of "d'" corresponds to the element of the matrix obtained in Eq. (4).

B. First-Order Parameters

Solving simultaneously Eqs. (2) and (6), we obtain the following equations for the values of the secondary and tertiary focal distances, f_2 and f_3:

$$f_2 = \frac{[(d_1 - f_1)F_{\text{total}} - (d_2 + d_w)f_1]}{[(d_1 - f_1 + d_2)F_{\text{total}} - (2d_2 + d_w)f_1]}, \quad (7)$$

$$f_3 = \frac{F_{\text{total}}(f_1 + d_2 + d_w - d_1)f_1 d_2^2}{Q}, \quad (8)$$

where

$$\begin{aligned} Q = {} & [F_{\text{total}}^2 + (F_{\text{total}} - d_w)2d_2 - d_2^2 - d_w^2]f_1^2 \\ & + [-F_{\text{total}}^2 d_1 + (-d_1 + d_2 + d_w)d_2 F_{\text{total}}]2f_1 \\ & + F_{\text{total}}^2 d_1^2. \end{aligned} \quad (9)$$

The diameters of the elements are obtained with the paraxial ray tracing. We evaluate Eqs. (7) and (8) proposing values for the total focal distance, F_{total}, the diameter, D_1, and the primary mirror focal distance, f_1, in addition to the pair of distances between the mirrors, d_1 and d_2.

The separations d_1 and d_2 must be selected in such a way that diminishes the vignetting produced by the primary and tertiary intersection D_3, in addition to the secondary diameter D_2, as is showed in Fig. 2.

C. Petzval Curvature

Korsch [1] and Robb [2] have shown three-mirror telescopes corrected for spherical, coma, and astigmatism in addition to Petzval curvature. We can control the Petzval curvature, P_c, minimizing the Petzval sum

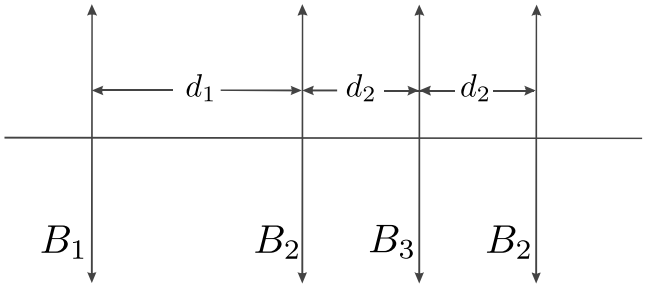

Fig. 1. Optical system representing the use of a third mirror with power $B_2 = 1/f_2$, where the light is reflected two times.

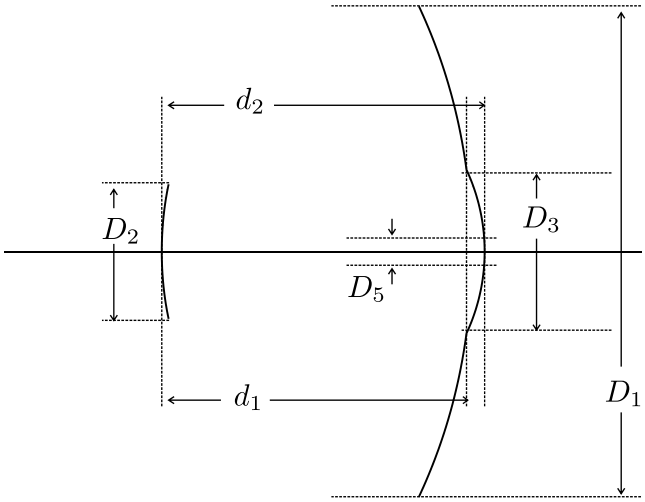

Fig. 2. Mirrors diameters and separations obtained by paraxial ray trace. The diameter D_4 is not shown in the figure because it corresponds to the second reflection through the secondary mirror where D_2 has been calculated.

$$P_c = \left(\frac{1}{f_1} + \frac{2}{f_2} + \frac{1}{f_3}\right). \tag{10}$$

The fact of minimizing the value of Eq. (10) does not mean that the proposed focal distances will generate a feasible asphericity. For this reason, we try to minimize it and do not necessarily obtain zero. Equation (10) implies that certain focal distances are negative, which leads to the obtainment of concave and convex surfaces.

3. Third-Order Design

The third-order aberrations coefficients [7] are defined by the Seidel sums, which are given by Eq. (11),

$$S_{\mathrm{I}} = -\sum_{k=0}^{n} A_k^2 h_k \Delta\left(\frac{u}{n}\right)_k, \tag{11a}$$

$$S_{\mathrm{II}} = -\sum_{k=0}^{n} A_k \bar{A}_k h_k \Delta\left(\frac{u}{n}\right)_k, \tag{11b}$$

$$S_{\mathrm{III}} = -\sum_{k=0}^{n} \bar{A}_k{}^2 h_k \Delta\left(\frac{u}{n}\right)_k, \tag{11c}$$

$$S_{\mathrm{IV}} = -\sum_{k=0}^{n} H_k^2 c_k \Delta\left(\frac{1}{n}\right)_k, \tag{11d}$$

$$S_{\mathrm{V}} = -\sum_{k=0}^{n} \left\{\frac{\bar{A}_k{}^3}{A_k} h_k \Delta\left(\frac{u}{n}\right)_k + \frac{\bar{A}_k}{A_k} H_k^2 c_k \Delta\left(\frac{1}{n}\right)_k\right\}. \tag{11e}$$

For systems with mirrors, the most commonly used convention set index $n = 1$ and $n' = -1$ before and after reflection means that for a ray traced from left to right and reflected backward makes the total optical path length positive.

$$L = \sum n_i l_i. \tag{12}$$

All the Gaussian parameters necessary to evaluate the Seidel sums were obtained from the first-order design.

A. Nomenclature

In the Seidel sums the following nomenclature is used.

The Lagrange invariant $H = \bar{h}A - h\bar{A}$, where $\bar{A}$ and A are the refraction invariants for a principal and a marginal ray, respectively. These are only invariants on a given surface. The Lagrange invariant is used in many ways: in the primary aberrations theory it is a measure of the light propagating through an optical system, making the connection between the principal ray and a ray through the center of the object.

In addition, $\bar{A} = n\bar{i}$ and $A = ni$, where i is the marginal ray angle and $\bar{i}$ is the principal ray angle, both for each element of the system $\bar{h}$ have to be considered. h corresponds to the principal ray height and the marginal ray for each surface. The refraction index is represented by n and the curvature of the elements by c, as is commonly used.

The value of $\Delta(u/n)_k$ is calculated by $(u_{k+1})/(n_{k+1}) - (u_k/n_k)$, and for $\Delta(1/n)_k$, we have $1/(n_{k+1}) - 1/(n_k)$. In addition, for Δn_k we will use $\Delta n_k = n_{k+1} - n_k$.

In optical systems, the value of c represents the inverse of the paraxial curvature of the surface. In reflective systems, the paraxial focal length of an element is given by one-half of its paraxial ratio, meaning

$$f = \frac{r_{\mathrm{Paraxial}}}{2} = \frac{1}{2c}. \tag{13}$$

B. Contribution of the Eccentricity

We intend to correct the system aberrations by means of conic surfaces, so we need modified Seidel coefficients. Equation [14] corresponds to the Seidel coefficients plus a contribution by the conic constant of the elements, $\varepsilon = -e^2$, where e^2 corresponds to the eccentricity.

$$S_{\mathrm{I}}^* = -\left[S_{\mathrm{I}} - \sum_{k=0}^{n} (\varepsilon_k c_k^3 h_k^4 \Delta n_k)\right], \tag{14a}$$

$$S_{\mathrm{II}}^* = -\left[S_{\mathrm{II}} - \sum_{k=0}^{n} (\varepsilon_k c_k^3 h_k^3 \bar{h}_k \Delta n_k)\right], \tag{14b}$$

$$S^*_{\mathrm{III}} = -\left[S_{\mathrm{III}} - \sum_{k=0}^{n}(\varepsilon_k c_k^3 h_k^2 \bar{h}_k^2 \Delta n_k)\right], \tag{14c}$$

$$S^*_{\mathrm{IV}} = -\left[S_{\mathrm{IV}} - \sum_{k=0}^{n}(\varepsilon_k c_k^3 h_k \bar{h}_k^3 \Delta n_k)\right]. \tag{14d}$$

C. Pupil Position Effect

The Seidel sums values depend on the pupil position [7] with respect to each optical element, as is shown in Eq. (15). The transmission invariant is modified with respect to the pupil position

$$\bar{A} = \frac{H}{h}(AhE - 1), \tag{15}$$

where

$$E_{k+1} - E_k = \frac{-d}{n h_k h_{k+1}}. \tag{16}$$

The value d represents the separation between the surfaces designated by k. In our case, the value is $E_0 = 0$ because the entrance pupil is located on the first surface. From Eqs. (11a), (15), and (16) we know that only the spherical aberration can be controlled by the three mirrors, and the contribution of the primary to the correction of coma and astigmatism is null. Coma and astigmatism can only be corrected by the secondary and tertiary mirrors. Notice how the value of $\bar{h}$ does not appear in the contribution for the spherical aberration in S^*_{I} [9].

D. System of Equations

To simplify, we can write $\alpha_i = c_i^3 h_i^4 \Delta n_k$, $\beta_i = c_i^3 h_i^3 \bar{h}_i \Delta n_k$, and $\gamma_i = c_i^3 h_i^2 \bar{h}_i{}^2 \Delta n_k$. With this simplification the first three coefficients of Eq. [14] become Eq. (17).

$$S^*_{\mathrm{I}} = -[S_{\mathrm{I}} - (\varepsilon_0\alpha_0 + \varepsilon_1\alpha_1 + \varepsilon_2\alpha_2 + \varepsilon_1\alpha_3)] = 0, \tag{17a}$$

$$S^*_{\mathrm{II}} = -[S_{\mathrm{II}} - (\varepsilon_1\beta_1 + \varepsilon_2\beta_2 + \varepsilon_1\beta_3)] = 0, \tag{17b}$$

$$S^*_{\mathrm{III}} = -[S_{\mathrm{III}} - (\varepsilon_1\gamma_1 + \varepsilon_2\gamma_2 + \varepsilon_1\gamma_3)] = 0. \tag{17c}$$

Therefore, we have three equations with three unknowns that can be solved to obtain the asphericity ε_0, ε_1, and ε_2 as shown below:

$$\varepsilon_0 = \frac{1}{\alpha_0}\left[S_{\mathrm{I}} + \frac{S_{\mathrm{III}}}{\delta}\xi - \frac{S_{\mathrm{II}}}{\delta}\mu\right], \tag{18a}$$

$$\varepsilon_1 = S_{\mathrm{II}}\frac{\gamma_2}{\delta} - S_{\mathrm{III}}\frac{\beta_2}{\delta}, \tag{18b}$$

$$\varepsilon_2 = S_{\mathrm{III}}\frac{\beta_1 + \beta_3}{\delta} - S_{\mathrm{II}}\frac{\gamma_1 + \gamma_3}{\delta}, \tag{18c}$$

where

$$\begin{aligned}\delta &= \beta_1\gamma_2 - \beta_2\gamma_1 - \beta_2\gamma_3 + \beta_3\gamma_2,\\ \xi &= \alpha_1\beta_2 - \alpha_2\beta_1 - \alpha_2\beta_3 + \alpha_3\beta_2,\\ \mu &= \alpha_1\gamma_2 - \alpha_2\gamma_1 - \alpha_2\gamma_3 + \alpha_3\gamma_2.\end{aligned} \tag{19}$$

4. Exact Design

In this section, we propose the algorithms used like functions in the exact corrections of the optical aberrations. Each intersection point $P(y,z)$ and director cosines (L,M,N) showed in this section were obtained by means of the exact ray tracing; the rest of the values are the same as those obtained in the first-order design. The only variables used in this Section is the asphericity ε_i. The algorithms for the ray trace and the correction are shown in Appendix A.

A. Spherical Aberration Correction

To correct the spherical aberration, we apply the Fermat's principle to the complete system. Figure 3 shows a marginal ray 4× reflected in the system. These four reflections have associated intersection points on each surface "i" given by $P(y_i, z_i)$. The final interception point has the dependences shown in Eq. (20), where c_i, ε_i, and d_i are the parameters of the elements and the separations, respectively.

$$p_{(y,z)_4} = p(c_1, c_2, c_3, d_1, d_2, d_3, \varepsilon_0, \varepsilon_1, \varepsilon_2, M, N). \tag{20}$$

Bearing in mind the points of intersection of the ray in Fig. 3, the total optical path for the marginal ray $\mathrm{OP}_{\mathrm{marginal}}$ is given by

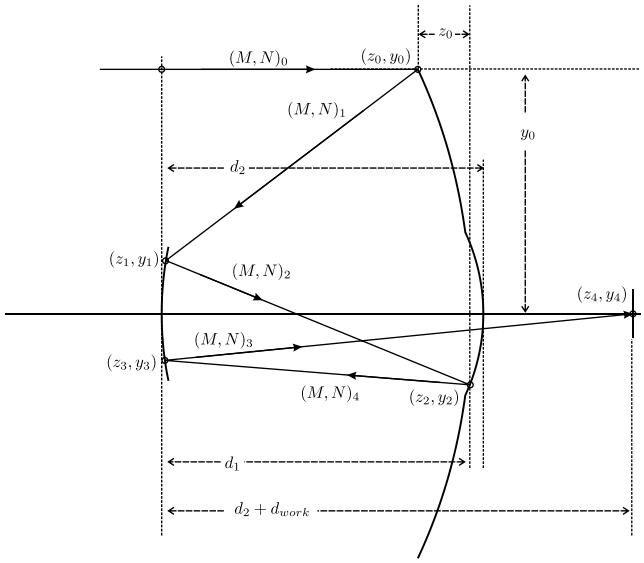

Fig. 3. Intersection points must be calculated with the exact ray trace for a marginal ray.

$$\begin{aligned}\mathrm{OP}_{\mathrm{marginal}} &= \sqrt{[z_0 - d_0]^2 + y_0]^2} \\ &+ \sqrt{[z_1 - z_0]^2 + [y_1 - y_0]^2} \\ &+ \sqrt{[z_2 - z_1]^2 + [y_2 - y_1]^2} \\ &+ \sqrt{[z_3 - z_2]^2 + [y_3 - y_2]^2} \\ &+ \sqrt{[z_4 - z_3]^2 + [y_4 - y_3]^2}.\end{aligned}$$

The optical path is a relation of the form $\mathrm{OP}_{\mathrm{marginal}}(\varepsilon_0, \varepsilon_1, \varepsilon_2)$. For a ray passing through the center of the entrance pupil, we have

$$\mathrm{OP}_{\mathrm{axis}} = d_0 + d_1 + d_2 + d_2 + (d_2 + d_w). \tag{21}$$

The Fermat's principle condition is represented by the equation

$$\mathrm{Fermat}(\varepsilon_0, \varepsilon_1, \varepsilon_2) = \mathrm{OP}_{\mathrm{marginal}} - \mathrm{OP}_{\mathrm{axis}} = 0. \tag{22}$$

B. Coma Aberration Correction

The function that corrects the coma aberration is based on the Abbe sine condition. We can get this function from the algorithm for the Fermat function, Eq. (22), because in Fig. 3, we have calculated the director cosines in each ray intersection when we built the Fermat function. The Abbe sine condition is given by Eq. (23) for an object at infinity, where the value of f_{Paraxial} is known beforehand. To get the value of the director cosine M_4, we need to find all the information about the marginal ray. This means that $M_4 = M_4(c_1, c_2, c_3, d_1, d_2, d_3, \varepsilon_1, \varepsilon_2, \varepsilon_3, L, M, N)$ or $M_4 = M_4(\varepsilon_1, \varepsilon_2, \varepsilon_3)$.

$$\mathrm{Abbe}(\varepsilon_1, \varepsilon_2, \varepsilon_3) = f_{\mathrm{Paraxial}} - \frac{y_0}{M_4} = 0. \tag{23}$$

C. Astigmatism Correction

In Fig. 4, a principal ray is used to find the intersection points on each surface. These intersection points were used to calculate the sagittal and tangential curvature ratios, r_s and r_t, with Eq. (24):

$$r_s = \frac{1}{c}\sqrt{(1 - \varepsilon c^2 y^2)}, \tag{24a}$$

$$r_t = \frac{1}{c}\sqrt{(1 - \varepsilon c^2 y^2)}^3. \tag{24b}$$

The sagittal and tangential positions, P_s and P_t, are given by the Coddington equations, Eq. (25). We should consider that objects and images are on the principal ray and not on the optical axis [8]. The calculation of Eq. (25) must be realized for each surface, considering that at first, the object is at infinity and subsequently at a finite position given by the image position after each element of the system.

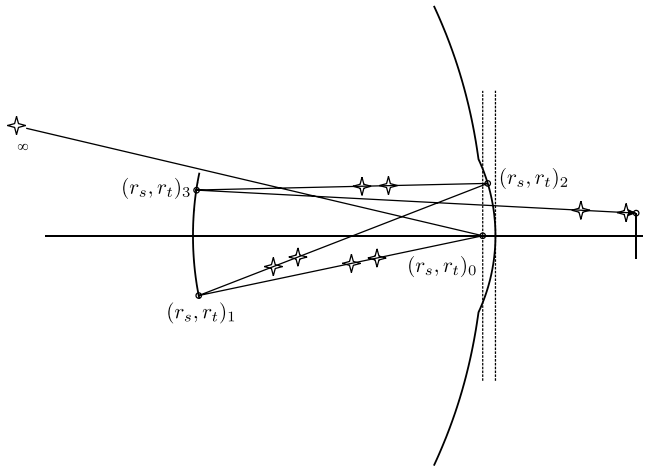

Fig. 4. Image of an object at infinity $P_s = \infty$ and $P_t = \infty$ is produced at finite positions by the mirrors in the telescope. The final sagittal position can be different from the tangential position because of astigmatism present in the system.

$$\frac{1}{P_{s'}} = \frac{2\cos I'}{r_s} - \frac{1}{P_s}, \tag{25a}$$

$$\frac{1}{P_{t'}} = \frac{2}{r_t \cos I'} - \frac{1}{P_t}. \tag{25b}$$

The intersection point on each surface of Fig. 4 was calculated by means of the exact ray tracing.

Again, the intersection points of the ray on the image surface are given by the form $p_{(x,y,z)} = p(c_1, c_2, c_3, d_1, d_2, d_3, \varepsilon_1, \varepsilon_2, \varepsilon_3, L, M, N)$. We can then consider that the image positions $P_{s'}$ and $P_{t'}$ are functions of $(\varepsilon_1, \varepsilon_2, \varepsilon_3)$, i.e., $P_{s_{\mathrm{final}}} = P_{s'}(\varepsilon_1, \varepsilon_2, \varepsilon_3)$ and $P_{t_{\mathrm{final}}} = P_{t'}(\varepsilon_1, \varepsilon_2, \varepsilon_3)$.

The final sagittal and tangential images are given by the final director cosine N and Eq. (26)):

$$f_{s_{\mathrm{final}}} = P_s(\varepsilon_1, \varepsilon_2, \varepsilon_3)N, \tag{26a}$$

$$f_{t_{\mathrm{final}}} = P_t(\varepsilon_1, \varepsilon_2, \varepsilon_3)N. \tag{26b}$$

Using these focal distances, we can build Eq. (27):

$$\mathrm{Coddington}(\varepsilon_0, \varepsilon_1, \varepsilon_2) = f_{S_{\mathrm{final}}} - f_{T_{\mathrm{final}}} = 0. \tag{27}$$

5. Design of an Anastigmatic and Compact Telescope

The three basic functions proposed in the previous sections represent three equations with three unknowns. It is impossible to find a simple analytic solution for the corresponding roots, ε; however, we can find the roots by means of a numerical method such as Newton–Raphson [10], which consists of finding the values for ε_1, ε_2, and ε_3 in Eq. (28) introducing

the values iteratively to refine the solution.

$$\begin{pmatrix} \varepsilon_0 \\ \varepsilon_1 \\ \varepsilon_2 \end{pmatrix} = \begin{pmatrix} \frac{df1}{d\varepsilon_0} & \frac{df1}{d\varepsilon_1} & \frac{df1}{d\varepsilon_2} \\ \frac{df2}{d\varepsilon_0} & \frac{df2}{d\varepsilon_1} & \frac{df2}{d\varepsilon_2} \\ \frac{df3}{d\varepsilon_0} & \frac{df3}{d\varepsilon_1} & \frac{df3}{d\varepsilon_2} \end{pmatrix}^{-1} \begin{pmatrix} f1 \\ f2 \\ f3 \end{pmatrix}. \quad (28)$$

To find the system roots with the Newton–Raphson method, it is necessary to select initial values, i.e., the first estimates for ε_0, ε_1, and ε_2. In this case, we have the previously found third-order solutions; we can use them as initial values.

To implement the Newton–Raphson method, it is necessary to know the derivatives of the functions to form the Jacobian. The derivatives are calculated numerically by Eq. (29):

$$\frac{df(\varepsilon)}{d\varepsilon} = \lim_{h\to 0} \frac{f(\varepsilon+h) - f(\varepsilon)}{h}. \quad (29)$$

The functions used in the Jacobian are the previously exhibited equations now renamed in the following way:

$$f1 = \text{Fermat}(\varepsilon_0, \varepsilon_1, \varepsilon_2), \quad (30a)$$

$$f2 = \text{Abbe}(\varepsilon_0, \varepsilon_1, \varepsilon_2), \quad (30b)$$

$$f3 = \text{Coddington}(\varepsilon_0, \varepsilon_1, \varepsilon_2). \quad (30c)$$

Table 1. Obtained Parameters

R (mm)	d (mm)	D (mm)	ε
−920	−347.74	150.00	−0.774
−1634.69	352.01	38.00	0.0
−329.93	−352.01	66.00	−0.396
−1634.69	352.01	30.22	0.0
171.00	−0.05	10.48	0

A. Example

To confirm the effectiveness of the proposed methodology, we designed a telescope using the following input parameters: $F_{\text{total}} = 2.4\,\text{m}$, $d_1 = 348\,\text{mm}$, $d_2 = 351.388\,\text{mm}$, and $D_1 = 300\,\text{mm}$. The field of view is 0.25°, and the working distance is $d_w = 100\,\text{mm}$. Examining values near $d_1 = 348\,\text{mm}$, we found that for $d_1 = 347.74\,\text{mm}$, the asphericity of the secondary mirror equals zero, making it is easier to polish. The results of the implemented algorithms with the proposed values are shown in Table 1.

The layout obtained with the values from Table 1 is presented in Fig. 5.

All the graphics shown in this example were obtained with the software Zemax [11]; the software was not used to optimize any parameter.

Figure 6 shows the resulting aberrations; we can see that the optical path difference is less than $\lambda/10$. The coma aberration is presented at the same scale.

In Fig. 7, the Petzval curvature was ignored to show the elimination of the astigmatism. The sagittal and tangential image planes are equal.

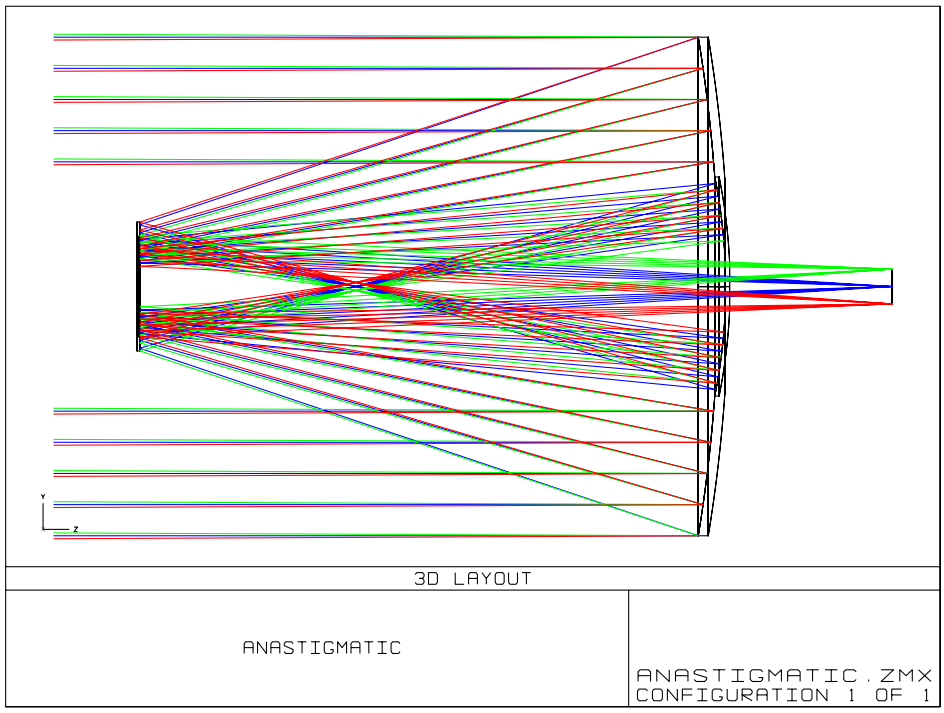

Fig. 5. (Color online) System layout.

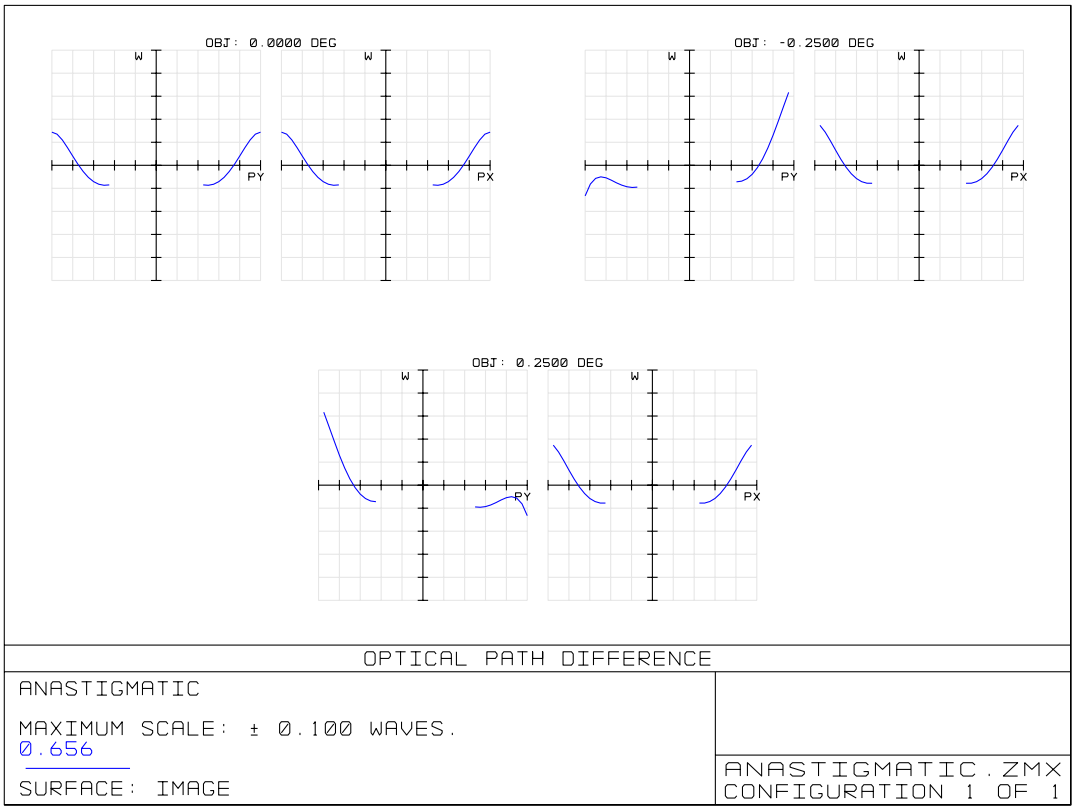

Fig. 6. (Color online) Aberrations obtained with the methodology shown in this work.

The spot diagram in the curved image plane is shown in Fig. 8, where we can see that the spot is less than the airy disk for the visible region of the spectrum; we can say that the system is diffraction limited.

In the same way, Figs. 7 and 8 show the spot diagrams without the contribution of the Petzval curvature. From the spot diagrams it is quite notable that the correction of the desired aberrations has been achieved.

6. Conclusions

The presented anastigmatic telescope is a compact solution for systems where a back focal length and good optical quality are required.

The analytical solutions for the third-order parameters are sufficiently good, and this is a good starting point to the exact parameters. The proposed design methodology is an alternative to the optimization process with optical design software.

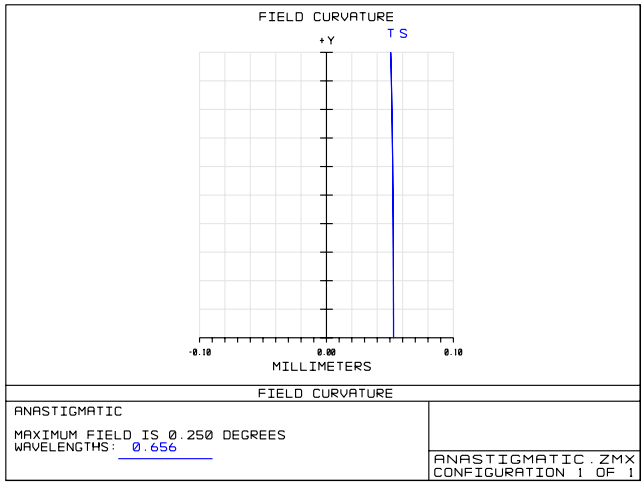

Fig. 7. (Color online) Sagittal and tangential image planes plotted on the image plane with Petzval curvature.

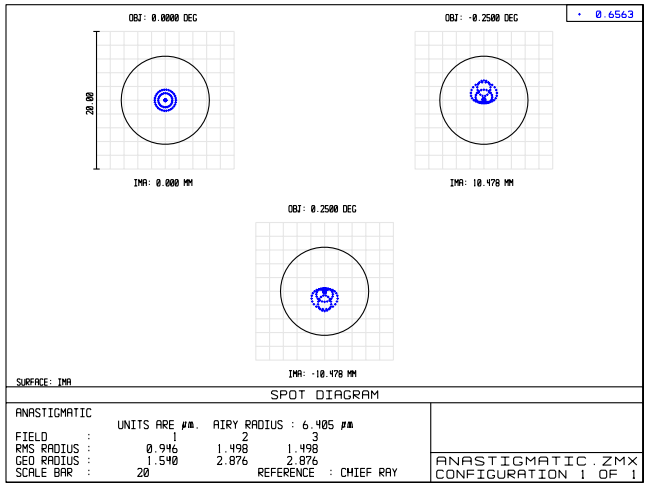

Fig. 8. (Color online) Spot diagram of the perfectly corrected system with an ideal image plane.

We can search for the best parameters to facilitate the construction, suitably choosing the entrance parameters such as diameters, separations, working distance, and power of the primary mirror.

The Petzval curvature given by the power of the elements is a problem that can be solved by means of the Petzval sum, Eq. (10).

Appendix A

The Appendix shows the exact ray trace used to construct the algorithms for the Fermat, Abbe, and Coddington functions.

The following, well known equations [6], are programed and executed in sequence through each element of the optical system. The ray trace shown in this Appendix is used for surfaces that can be represented by the general quadratic of revolution equation:

$$z = \frac{1}{2}c(x^2 + y^2 + \varepsilon z^2), \tag{A1}$$

where ε is the asphericity and c is the inverse of the paraxial ratio (also known as curvature).

The entrance parameters are the initial position of the ray (x, y, z), the director cosines (L, M, N), and the distance to the vertex of the next surface. The following three equations are the intersection points of a ray in a plane that is in the vertex of the next surface.

$$x_0 = x_{-1} + \frac{L}{N}(d - z_{-1}). \tag{A2}$$

$$y_0 = y_{-1} + \frac{M}{N}(d - z_{-1}). \tag{A3}$$

Values F and G are simplifications to shorten the following equations:

$$F = c(x_0^2 + y_0^2), \tag{A4}$$

$$G = N - c(Lx_0 + My_0). \tag{A5}$$

The value of Δ is the separation between the plane in the vertex of the surface and the intersection point of the ray. Now, we need the characteristics of the optical surface such as asphericity ε and curvature c.

$$\Delta = \frac{F}{G + \sqrt{G^2 - cF[1 + (\varepsilon - 1)N^2]}}. \tag{A6}$$

The next three equations are the intersection points mentioned earlier.

$$x = x_0 + L\Delta. \tag{A7}$$

$$y = y_0 + M\Delta. \tag{A8}$$

$$z = N\Delta. \tag{A9}$$

Applying Snell's law to the ray in the intersection point, the following equations are written in general form and work well for refractions or reflections through any system, taking a few considerations.

$$J = \sqrt{1 - 2c(\varepsilon - 1)z + c^2\varepsilon(\varepsilon - 1)z^2}. \tag{A10}$$

$$\cos I = \frac{\sqrt{G^2 - cF[1 + (\varepsilon - 1)N^2]}}{J}. \tag{A11}$$

$$n' \cos I' = \sqrt{n'^2 - n^2(1 - \cos I^2)}. \tag{A12}$$

$$K = c(n' \cos I' - n \cos I). \tag{A13}$$

The resulting director cosines after reflection or refraction are given by

$$L' = \frac{1}{n'}\left[nL - \frac{Kx}{J}\right], \tag{A14}$$

$$M' = \frac{1}{n'}\left[nM - \frac{Ky}{J}\right], \tag{A15}$$

$$N' = \frac{1}{n'}\left[nN + \frac{(1 - z\varepsilon c)K}{Jc}\right]. \tag{A16}$$

For reflective systems in air, we must set a refraction index $n = -1$ prior to the reflection and $n = 1$ after the reflection.

The Fermat, Abbe, and Coddington functions were constructed using the ray's intersection on each surface i. The calculation of the coordinates (x, y, z) requires the evaluation from Eqs. (A2)–(A16), thus every coordinate is represented in terms of its dependencies, as follows:

$$x_i = x(x_{i-1}, y_{i-1}, z_{i-1}, c_i, d_i, \varepsilon_i, L_i, M_i, N_i), \tag{A17}$$

$$y_i = y(x_{i-1}, y_{i-1}, z_{i-1}, c_i, d_i, \varepsilon_i, L_i, M_i, N_i), \tag{A18}$$

$$z_i = z(x_{i-1}, y_{i-1}, z_{i-1}, c_i, d_i, \varepsilon_i, L_i, M_i, N_i). \tag{A19}$$

The following algorithms were programed using Mathcad software [12].

The exact ray trace was programed in a function called Exax, which depends on a vector $PV = (x, y, z, L, M, N)$. The Fermat, Abbe, and Coddington functions use the Exax function to find the required intersection points throughout the system.

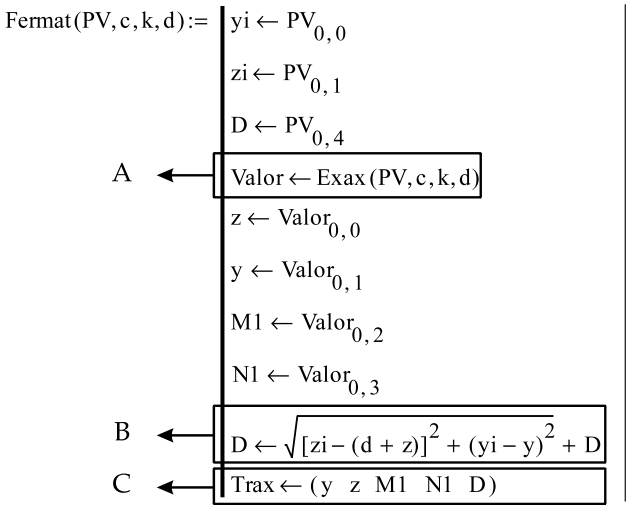

Fig. 9. Fermat algorithm.

Figure 9 shows the Fermat algorithm, which calculates the optical path between surfaces; Fig. 10 applies this algorithm through the system's surfaces to obtain the total optical path difference (OPD).

A represents the use of the Exax function in order to obtain the exact ray trace, *B* calculates the optical path, and *C* is the exit vector, which in addition contains the optical path *D*.

For the algorithm shown in Fig. 10, *A* applies the Fermat algorithm using the contribution of each surface until reaching the image plane. *B* calculates the optical path for a ray on the optical axis, and *C* calculates the OPD, Eq. (22).

The algorithm Coma (Fig. 11) uses the Fermat algorithm (*A*) to obtain the director cosine for a ray exiting the system, and *B* represents Eq. (23).

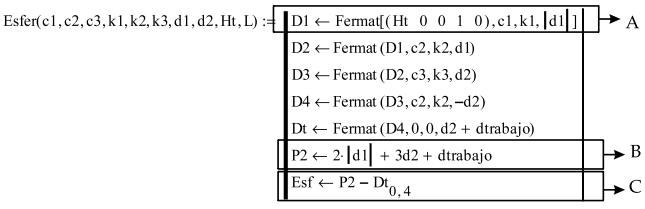

Fig. 10. Esfer algorithm.

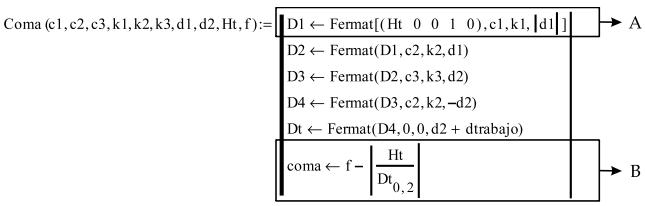

Fig. 11. Coma algorithm.

Figure 12, shows the algorithm Codd. Points *A* to *E* are used to calculate the sagittal and tangential focal lengths, (Eqs. (24) and (25)).

Finally, algorithm Astig shown in Fig. 13, calculates the final sagittal and tangential focal lengths to evaluate Eq. (27).

Eq. (A20) represent the principles in Eqs. (22), (23), and (27). The functions f_1, f_2, and f_3 must be solved for the values of x_1, x_2, and x_3, which are

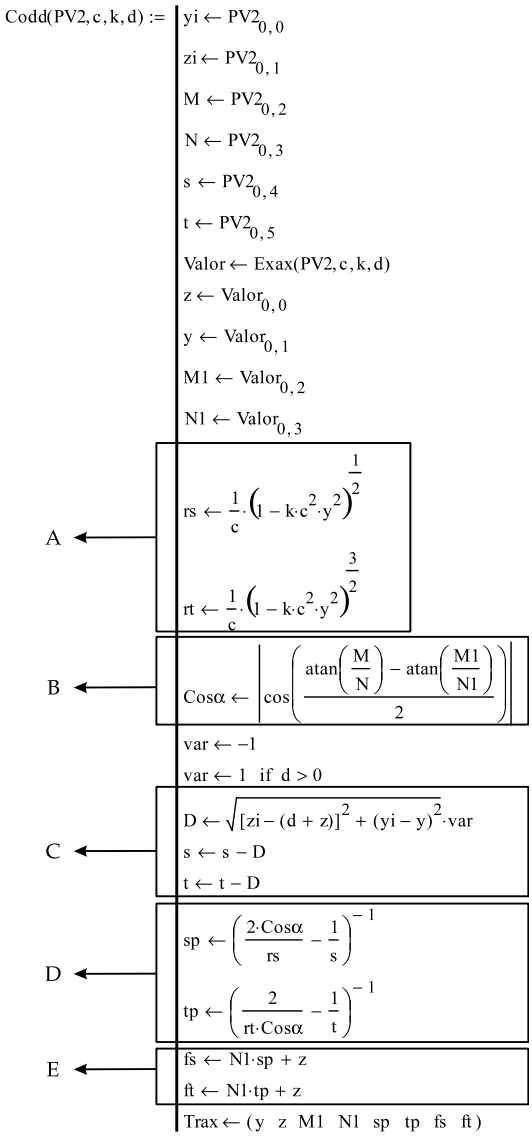

Fig. 12. Codd algorithm.

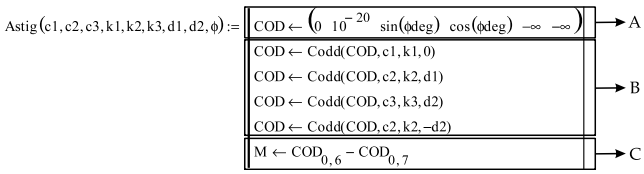

Fig. 13. Astig algorithm.

the asphericities.

$$f_1(x_1,x_2,x_3) = \mathrm{Esfer}(c_1,c_2,c_3,x_1,x_2,x_3,d_1,d_2,H_t,L),$$
$$f_2(x_1,x_2,x_3) = \mathrm{Coma}(c_1,c_2,c_3,x_1,x_2,x_3,d_1,d_2,H_t,f),$$
$$f_3(x_1,x_2,x_3) = \mathrm{Astig}(c_1,c_2,c_3,x_1,x_2,x_3,d_1,d_2,\theta). \tag{A20}$$

We thank W. J. Schuster for carefully reading the final manuscript.

References

1. D. Korsch, "Anastigmatic three-mirror telescope," Appl. Opt. **16**, 2074–2077 (1977).
2. P. N. Robb, "Three-mirror telescopes: design and optimization," Appl. Opt. **17**, 2677–2685 (1978).
3. L. G. Seppala, "Improved optical design for the large synoptic survey telescope (lsst)," Proc. SPIE **4836**, 111–118 (2002).
4. V. Draganov, "Compact telescope," U.S. Patent 6,667,831 (23 December 2003).
5. A. Gerrard and J. M. Burch, *Introduction to Matrix Methods in Optics* (Dover, 1994), Chap. 1.
6. W. Welford, *Aberrations of Optical Systems*, Series on Optics and Optoelectronics, 1st ed. (Taylor and Francis, 1986), Chaps. 6, 4, 8.
7. M. J. Kidger, ed., *Fundamental Optical Design*, Vol. PM92 of SPIE Press Monograph Series (SPIE, 2001), pp. 101–164, Chaps. 6, 7.
8. W. Smith, *Modern Optical Engineering*, 4th ed. (McGraw-Hill, 2007), Chap. 10.
9. D. Korsch, *Reflective Optics* (Academic, 1991), Chap. 9.
10. W. Cheney and D. Kindcaid, *Numerical Mathematics and Computing*, 6th ed. (Thomson Brooks/Cole, 2008), Chap. 3.
11. URL: www.zemax.com.
12. URL: http://www.ptc.com/products/mathcad/.